Automated Exploration of Adsorption Structures of an Organic Molecule on RuH_2−BINAP by the ONIOM Method and the Scaled Hypersphere Search Method

Satoshi Maeda and Koichi Ohno*

Department of Chemistry, Graduate School of Science, Tohoku University, Aramaki, Aoba-ku, Sendai 980-8578, Japan

Received: October 10, 2007

Automated exploration of adsorption structures of a molecule ($CH_3COCH_2COOCH_3$) on an organometallic complex of (*R*)-RuH_2−BINAP (BINAP = 2,2′-bis(diphenylphosphino)-1,1′-binaphthyl) has been performed by a combination of the ONIOM method and the scaled hypersphere search (SHS) method. As many as 135 potential minima have been obtained as candidates of adsorption structures. The most stable structure among the 135 is a precursor of the (*R*)-type product, which is about 30 kJ/mol more stable than the most stable structure among precursors of the (*S*)-type product. This unbiased search is theoretically showing the power of BINAP to distinguish (*R*)-type and (*S*)-type at the adsorption state. This result is in line with very high optical yield of the (*R*)-type product in the corresponding experiment.

1. Introduction

Transition metal complex mediated chemical processes have been studied by using small model systems,[1] because of (1) huge computation demands for potential energy calculations of many-electron (real) systems and (2) high dimensionality of potential energy surfaces (PES) in many-variable (real) systems. Recent developments of QM/MM (quantum mechanics/molecular mechanics) hybrid methods such as the ONIOM[2] method have improved the former problem, and steric effects of large ligands can directly be taken into account in geometry optimizations.[3]

There have been considerable efforts of developments of efficient tools for exploration on the PES,[4] and such techniques have also been employed in transition-metal-involved systems.[5] However, systematic and automatic methods have only been applied to empirical model potentials of very large systems; hence, equilibrium structures (EQ) and transition state structures (TS) of large organometallic systems, which cannot be dealt with by simple model potentials, have been examined by geometry optimizations starting from limited numbers of initial guesses based on intuitions or experiences of researchers.

Recently, we proposed the anharmonic downward distortion (ADD) following by the scaled hypersphere search (SHS) method for efficient exploration on quantum chemical PES.[6] Although there has been no general method to follow reaction pathways starting from an EQ toward the TSs, the SHS method made it possible. The full ADD (FADD) following enables us to obtain the global reaction route map (GRRM) on the PES,[6] while lower energy parts of the PES connected via low-barrier pathways can be explored very quickly by the large ADD (LADD) following.[7] In this paper, we demonstrate that structures of organometallic systems can be explored systematically and automatically by a combination of the ONIOM method and the LADD following by the SHS method.

The BINAP (2,2′-bis(diphenylphosphino)-1,1′-binaphthyl) transition metal complex developed by Noyori et al. has been employed in asymmetric syntheses of many chiral molecules with very high enantioselectivity.[8,9] Although the microscopic role of BINAP in asymmetric hydrogenations has been extensively studied both experimentally[10] and theoretically,[11] its mechanism and the origin of such high selectivity are still important subjects of research.[12] BINAP has four phenyl groups, and steric effects between these ligands and the adsorbing organic molecule can yield many isomers of adsorption structures. Hence, a thorough search for such isomers may be very interesting for further understanding on BINAP's role as well as for the first application of the present approach.

2. Model System

Although most previous computational studies focus on reactions of BINAP−Rh(I),[11,12] there have been extensive experimental studies on hydrogenation mechanisms of BINAP−Ru(II).[10] The first step of hydrogenation reactions by BINAP−Ru(II) is substitution of one of the anion ligands in RuL_2−BINAP by a H atom via a reaction with H_2 yielding RuHL−BINAP and HL, where $OCOCH_3$, Cl, Br, I, etc. are used as anion ligands of L. The second step is coordination of the reactant molecule onto the catalysis of RuHL−BINAP, which is the main topic of this paper.

In this study, coordination of $CH_3COCH_2COOCH_3$ onto RuH_2−BINAP is considered, where L = H is chosen as the simplest case. Enantioselectivity of BINAP−Ru(II) strongly depends on the choice of anion ligands.[10] In the case of the asymmetric hydrogenation reaction of $CH_3COCH_2COOCH_3$,[13] $Ru(OCOCH_3)_2$−BINAP results in very low optical yield, whereas $RuCl_2$−BINAP shows very high selectivity of more than 99% ee. Hence, a series of studies using different L may be required for systematic understanding on the role of L; we start from the simplest case of L = H in this first application of the ONIOM−SHS combination approach.

3. Method

3.A. Scaled Hypersphere Search Method. The SHS method is an uphill walking technique on a PES starting from an EQ

---

* Corresponding author. Tel.: +81-22-795-6576. Fax: +81-22-795-6580. E-mail: ohnok@qpcrkk.chem.tohoku.ac.jp.

10.1021/jp709874f CCC: $37.00

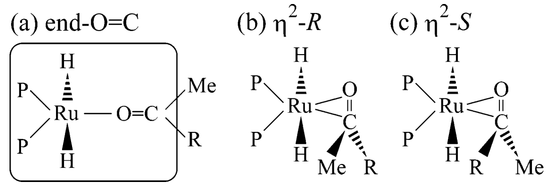

Figure 1. Schematic illustrations of (a) end-coordination (C═O: → Ru) complex denoted as (end-O═C)-type, (b) η^2-coordination complex (a precursor of (*R*)-type product) denoted as (η^2-*R*)-type, and (c) η^2-coordination complex (a precursor of (*S*)-type product) denoted as (η^2-*S*)-type, where Me and R indicate methyl group and CH_2COOCH_3 group, respectively. The square in (a) shows atoms treated by QM (DFT) calculations in the ONIOM method.

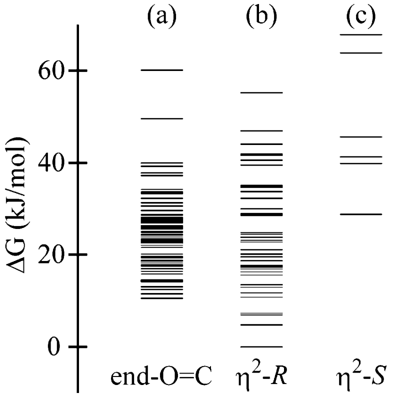

Figure 2. Relative free energies (at 373.15 K) of (a) 78 (end-O═C)-type structures, (b) 46 (η^2-*R*)-type structures, and (c) 6 (η^2-*S*)-type structures. See Figure 1 for definition of each type.

toward TSs or dissociation channels (DC).[6] Since typical reaction paths always change their curvatures from concave to convex on going to a TS or a DC, slopes should always decline their inclinations downward from a respective harmonic curve because of energy-lowering interactions leading to a TS or a DC. The SHS method follows such an anharmonic effect, i.e., ADD, as a symptom of a chemical reaction starting from an EQ toward a TS or a DC. Directions containing the maximal ADD can be detected as energy minima on the isoenergy hypersurface of harmonic potential. Although this hypersurface is a hyperellipsoid when usual normal coordinates Q_i are employed, it can be transformed into a simple hypersphere by using the scaled normal coordinates q_i, where all normal coordinates Q_i are scaled by corresponding eigenvalues λ_i as $q_i = \lambda_i^{1/2}Q_i$. This transformation reduces an algorithm of ADD following to energy minimizations on a series of different sizes of scaled hyperspheres with expanding their radii.

The ADD following by the SHS method can be used for finding many reaction pathways around an EQ, and global reaction route mapping on a quantum chemical PES can be performed in an automatic way when all possible reaction pathways leading ADDs are followed starting from all obtained EQs in a process.[6] Although this FADD following has successfully been applied to small systems with 4−12 atoms,[6,14] its application to larger systems including more than 20 atoms may not be straightforward because of the high-dimensionality problem. Therefore, we recently introduced some simplifications to quickly explore low-energy parts of the PES connected via low-barrier pathways.[7] The most important point in the simplification is use of LADD following in which only large ADDs are followed as important pathways leading to lower energy EQ via a low barrier. Applications of this LADD following to ab initio PESs of H-bond cluster systems have been successful to reproduce recent experimental observations[15] as well as extensive Monte Carlo simulations based on model potentials.[7] In this study, we combined this LADD following with the ONIOM method to automatically explore adsorption structures of an organic molecule on an organometallic complex.

3.B. Computations. In the ONIOM calculation, the carbonyl which will be hydrogenated, the Ru atom, H atoms bonded to the Ru atom, and P atoms were dealt with QM, as the simplest model, and C atoms bonded to these QM atoms were replaced by a H atom in QM calculations (see Figure 1a for illustration of the QM part). The MM part was treated by the universal force field,[16] where partial charges on each atom were estimated by the QEq method[17] at separately optimized geometries of RuH_2−BINAP and the reactant molecule. The QM part was treated by the density functional theory based on the B3LYP functional,[18] where the 6-31G basis set was employed for H, C, and O atoms, and the LANL2DZ basis set and its effective core potential was applied to Ru and P atoms. The search by the SHS method was started from an end-coordination structure (C═O: → Ru) obtained by geometry optimization. All 285 vibrational freedoms were considered in the search. In the LADD following by the SHS method, nine ADDs were detected around each EQ to follow the largest three ADDs. In total, 175 adsorption structures were automatically located by the SHS method in application to the ONIOM PES. Then, these structures were reoptimized using the 6-311++G** basis set for H, C, O, and P atoms, and 135 structures were confirmed to be independent potential energy minima on the PES. Zero-point energy and free energy correction at 373.15 K were estimated by harmonic approximation of the PES in the gas phase. The Boltzmann distribution of each structure was further estimated by using the free energy values for qualitative discussions. All calculations were made by using a developing version of the GRRM program[6,7] in which energy, gradient, and Hessian based on the ONIOM method were calculated by the GAUSSIAN03 programs.[19]

4. Results and Discussion

As a result, 135 adsorption structures (potential minima) have been obtained. Among these 135 structures, most of them can be assigned to one of three types illustrated in Figure 1a−c. Figure 1a shows an illustration of the end-coordination structures (C═O: → Ru) via a lone-pair of an O atom, and 76 structures among the 135 are of this (end-O═C) type. Figure 1, parts b and c, shows illustrations of η^2-coordination structures via the π orbital of the carbonyl. Such η^2-coordination structures can further be classified into two types of (Figure 1b) a precursor of the (*R*)-type product denoted as (η^2-*R*)-type or (Figure 1c) a precursor of the (*S*)-type product denoted as (η^2-*S*)-type, because hydrogen atoms on the Ru atom can approach only from one side of the carbonyl. Among 135 structures, 46 are (η^2-*R*)-type and 6 are (η^2-*S*)-type.

Figure 2 depicts free energy distributions of (Figure 2a) (end-O═C)-type structures, (Figure 2b) (η^2-*R*)-type structures, and (Figure 2c) (η^2-*S*)-type structures. As can be seen from Figure 2, most low-lying structures are (η^2-*R*)-type; in contrast, (η^2-*S*)-type structures are in the high-energy region, which is demonstrating the power of (*R*)-RuH_2−BINAP to distinguish (η^2-*R*)-type and (η^2-*S*)-type. This result has been obtained by an unbiased search starting from one of the (end-O═C)-type structures. Here, (η^2-*R*)-type and (η^2-*S*)-type are not connected by a direct reaction route but connected by pathways via (end-O═C)-type. The LADD following by the SHS method prefers to go through low-barrier pathways involving large ADD, and therefore the present results are indicating that there are lots of

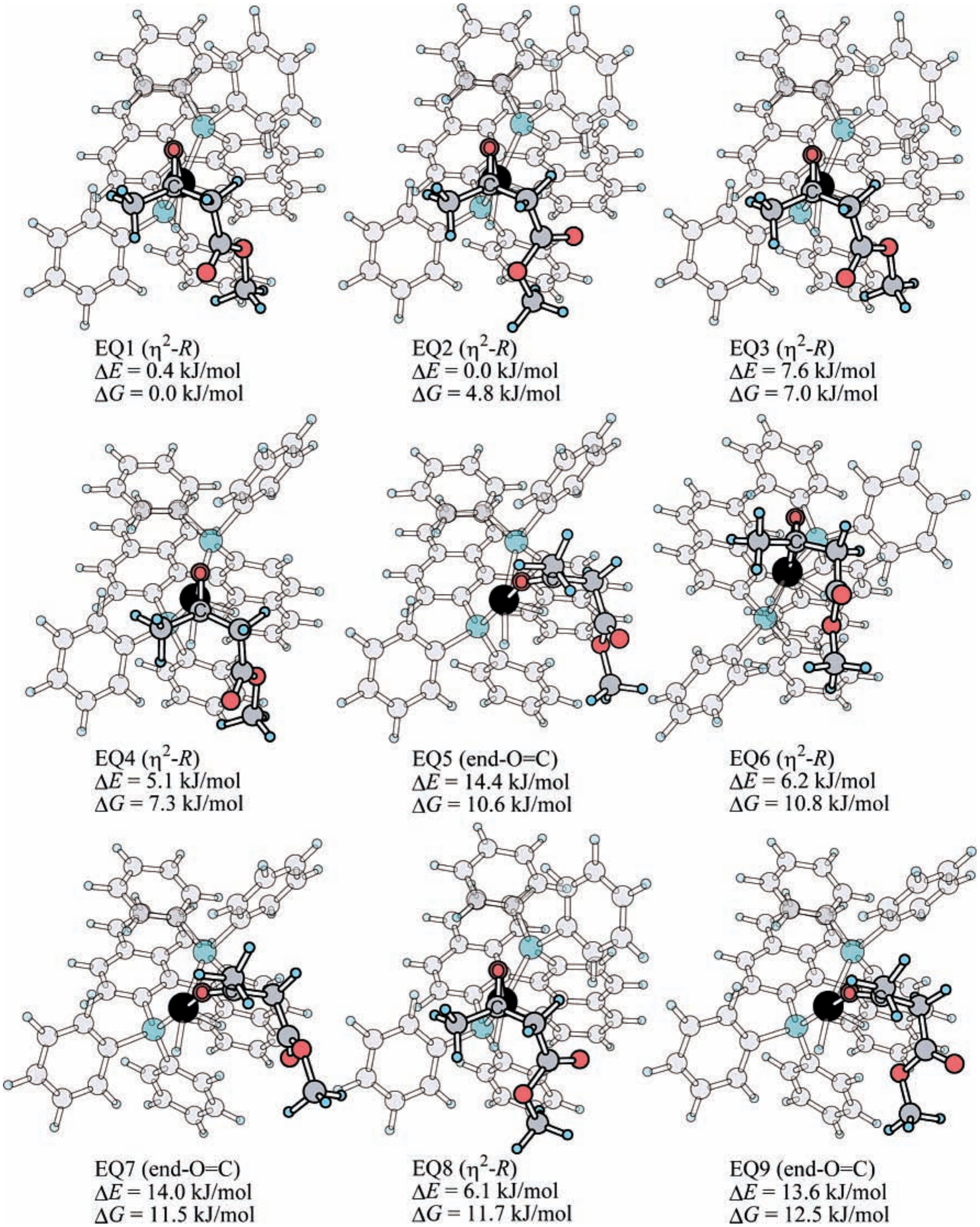

EQ1 (η^2-*R*)
$\Delta E = 0.4$ kJ/mol
$\Delta G = 0.0$ kJ/mol

EQ2 (η^2-*R*)
$\Delta E = 0.0$ kJ/mol
$\Delta G = 4.8$ kJ/mol

EQ3 (η^2-*R*)
$\Delta E = 7.6$ kJ/mol
$\Delta G = 7.0$ kJ/mol

EQ4 (η^2-*R*)
$\Delta E = 5.1$ kJ/mol
$\Delta G = 7.3$ kJ/mol

EQ5 (end-O=C)
$\Delta E = 14.4$ kJ/mol
$\Delta G = 10.6$ kJ/mol

EQ6 (η^2-*R*)
$\Delta E = 6.2$ kJ/mol
$\Delta G = 10.8$ kJ/mol

EQ7 (end-O=C)
$\Delta E = 14.0$ kJ/mol
$\Delta G = 11.5$ kJ/mol

EQ8 (η^2-*R*)
$\Delta E = 6.1$ kJ/mol
$\Delta G = 11.7$ kJ/mol

EQ9 (end-O=C)
$\Delta E = 13.6$ kJ/mol
$\Delta G = 12.5$ kJ/mol

Figure 3. Nine lowest energy structures (in terms of free energy at 373.15 K) among 135 structures obtained by the present search. Coordination types according to the definition in Figure 1 are shown in parentheses. ΔE and ΔG show potential energy value and free energy (at 373.15 K) value, respectively, relative to the lowest ones.

low-barrier pathways from (end-O═C)-type to (η^2-*R*)-type but few pathways to (η^2-*S*)-type. It follows that the smaller number of (η^2-*S*)-type structures in the present results is also due to the characteristic of (*R*)-RuH_2−BINAP to prefer (η^2-*R*)-type.

To look into the reason why (*R*)-RuH_2−BINAP prefers (η^2-*R*)-type, we discuss the obtained structures in detail. Figure 3 shows the nine lowest structures (in terms of free energy at 373.15 K) including six (η^2-*R*)-type structures and three (end-O═C)-type ones. In most of the stable (η^2-*R*)-type structures, one phenyl group projecting forward is interacting with a less bulky methyl group and a bulky CH_2COOCH_3 group is interacting with another phenyl group lying backward, and such an arrangement is minimizing steric repulsion between $CH_3COCH_2COOCH_3$ and (*R*)-RuH_2−BINAP. In short, these structures can be regarded to be the “lock-and-key” motif where (*R*)-RuH_2−BINAP is a lock and $CH_3COCH_2COOCH_3$ is a key. Figure 4 shows the most stable structure among the (η^2-*S*)-type, which is the 94th lowest (in terms of free energy at 373.15 K) among all 135 structures. In this (η^2-*S*)-type structure, the bulky CH_2COOCH_3 group is interacting with a phenyl group projecting forward, and this stronger steric repulsion makes the (η^2-*S*)-type structure unstable relative to (η^2-*R*)-type ones. In the present search, steric effects have successfully been taken into account by the ONIOM method, and the special stability of (η^2-

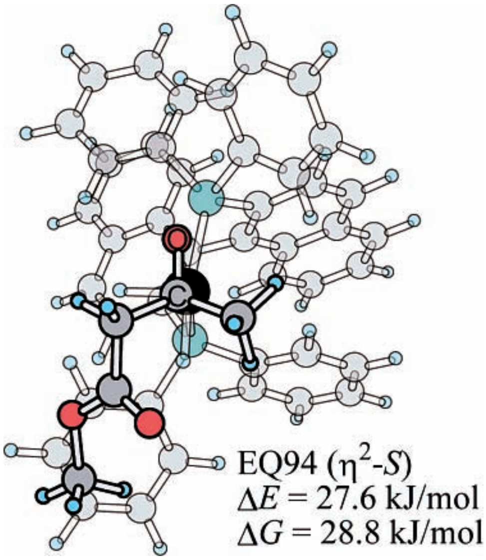

Figure 4. Lowest energy adsorption structure (in terms of free energy at 373.15 K) among (η^2-*S*)-type structures.

R)-type structures due to the “lock-and-key” motif could automatically be discovered by the SHS method. It should be noted that the present search is including coordination bond rearrangement events of isomerization among (η^2-*R*), (end-O═C), and (η^2-*S*) types, which is difficult to describe by pure MM approaches. Hence, the present ONIOM−SHS combination rather than MM−SHS combination may be of great significance for proper understanding on adsorption structures of this system.

The ratio of Boltzmann distributions at 373.15 K of (η^2-*R*)-type structures and (η^2-*S*)-type ones is estimated as 1.00:0.00, which indicates that enantioselectivity of this reaction may be 100% ee when instantaneous equilibration is assumed in the adsorption state. This value will change depending on the choice of anion ligands[10] and/or adsorbing molecule,[13] and systematic applications of the present approach to different sets of anion ligands and adsorbing molecule may be a next interest. Of course, other points such as reaction barriers should also be very important for microscopic understanding on the role of asymmetric hydrogenation catalysis,[12,20] and applications of the ONIOM−SHS combination to such processes are in progress.

We finally note about the computation costs of the present calculations. The present calculations required about 10^5 times ONIOM force calculations, which have taken about 1 month by using two cores in only one CPU (Xeon, 3.00 GHz). It follows that the present ONIOM−SHS combination can routinely be applied to similar systems, and it may be promising for systematic understanding on adsorption structures of an organic molecule onto an organometallic complex with large ligands.

5. Conclusions

This paper shows the first application of the ONIOM−SHS combination approach to an organometallic system. The ONIOM−SHS method gave as many as 135 potential minima as candidates of adsorption structures of $CH_3COCH_2COOCH_3$ on (*R*)-RuH$_2$−BINAP. The most stable structure among the 135 is an η^2-coordination complex which can be regarded to be a precursor of the (*R*)-type product. The special stability of this structure can be explained by the “lock-and-key” motif, and it is 28.8 kJ/mol more stable than the most stable structure among precursors of the (*S*)-type product. The present result is in line with the very high enantioexcess of the (*R*)-type product in the corresponding experiment and theoretically shows the power of BINAP to distinguish (*R*)-type and (*S*)-type at the adsorption state. The present ONIOM−SHS combination approach may be promising for systematic understanding on adsorption structures of an organic molecule onto an organometallic complex with large ligands.

Acknowledgment. S. Maeda is supported by a Research Fellowship of the Japan Society for Promotion of Science for Young Scientists. The authors thank Dr. Yi Luo for helpful discussions.

References and Notes

(1) Reviews: (a) Koga, N.; Morokuma, K. *Chem. Rev.* **1991**, *91*, 823. (b) Niu, S.; Hall, M. B. *Chem. Rev.* **2000**, *100*, 353. (c) Torrent, M.; Solà, M.; Frenking, G. *Chem. Rev.* **2000**, *100*, 439.

(2) (a) Svensson, M.; Humbel, S.; Froese, R. D. J.; Matsubara, T.; Sieber, S.; Morokuma, K. *J. Phys. Chem.* **1996**, *100*, 19357. (b) Dapprich, S.; Komáromi, I.; Byun, K. S.; Morokuma, K.; Frisch, M. J. *THEOCHEM* **1999**, *461−462*, 1. (c) Vreven, T.; Morokuma, K. *J. Comput. Chem.* **2000**, *21*, 1419. (d) Vreven, T.; Morokuma, K.; Farkas, Ö.; Schlegel, H. B.; Frisch, M. J. *J. Comput. Chem.* **2003**, *24*, 760.

(3) Torrent, M.; Vreven, T.; Musaev, D. G.; Morokuma, K.; Farkas, Ö.; Schlegel, H. B. *J. Am. Chem. Soc.* **2002**, *124*, 192.

(4) Review: Schlegel, H. B. *J. Comput. Chem.* **2003**, *24*, 1514.

(5) Review: Ziegler, T.; Autschbach, J. *Chem. Rev.* **2005**, *105*, 2695.

(6) (a) Ohno, K.; Maeda, S. *Chem. Phys. Lett.* **2004**, *384*, 277. (b) Maeda, S.; Ohno, K. *J. Phys. Chem. A* **2005**, *109*, 5742. (c) Ohno, K.; Maeda, S. *J. Phys. Chem. A* **2006**, *110*, 8933.

(7) Maeda, S.; Ohno, K. *J. Phys. Chem. A* **2007**, *111*, 4527.

(8) Noyori, R. *Asymmetric Catalysis in Organic Synthesis*; Wiley: New York, 1994.

(9) Review: Noyori, R. *Angew. Chem., Int. Ed.* **2002**, *41*, 2008.

(10) Review: Noyori, R.; Kitamura, M.; Ohkuma, T. *Proc. Natl. Acad. Sci. U.S.A.* **2004**, *101*, 5356.

(11) Review: Gridnev, I. D.; Imamoto, T. *Acc. Chem. Res.* **2004**, *37*, 633.

(12) Mori, S.; Vreven, T.; Morokuma, K. *Chem. Asian J.* **2006**, *1*, 391.

(13) (a) Kitamura, M.; Tokunaga, M.; Ohkuma, T.; Noyori, R. *Org. Synth. Collect.* **1998**, *9*, 589. (b) Kitamura, M.; Tokunaga, M.; Ohkuma, T.; Noyori, R. *Org. Synth. Collect.* **1993**, *71*, 1.

(14) (a) Yang, X.; Maeda, S.; Ohno, K. *J. Phys. Chem. A* **2005**, *109*, 7319. (b) Yang, X.; Maeda, S.; Ohno, K. *Chem. Phys. Lett.* **2006**, *418*, 208. (c) Yang, X.; Maeda, S.; Ohno, K. *J. Phys. Chem. A* **2007**, *111*, 5099. (d) Watanabe, Y.; Maeda, S.; Ohno, K. *Chem. Phys. Lett.* **2007**, *447*, 21.

(15) Luo, Y.; Maeda, S; Ohno, K. *J. Phys. Chem. A* **2007**, *111*, 10732.

(16) Rappé, A. K.; Casewit, C. J.; Colwell, K. S.; Goddard., W. A., III; Skiff, W. M. *J. Am. Chem. Soc.* **1992**, *114*, 10024.

(17) Rappé, A. K.; Goddard, W. A., III. *J. Phys. Chem.* **1991**, *95*, 3358.

(18) Becke, A. D. *J. Chem. Phys.* **1993**, *98*, 5648.

(19) Frisch, M. J.; Trucks, G. W.; Schlegel, H. B.; Scuseria, G. E.; Robb, M. A.; Cheeseman, J. R.; Montgomery, J. A., Jr.; Vreven, T.; Kudin, K. N.; Burant, J. C.; Millam, J. M.; Iyengar, S. S.; Tomasi, J.; Barone, V.; Mennucci, B.; Cossi, M.; Scalmani, G.; Rega, N.; Petersson, G. A.; Nakatsuji, H.; Hada, M.; Ehara, M.; Toyota, K.; Fukuda, R.; Hasegawa, J.; Ishida, M.; Nakajima, T.; Honda, Y.; Kitao, O.; Nakai, H.; Klene, M.; Li, X.; Knox, J. E.; Hratchian, H. P.; Cross, J. B.; Adamo, C.; Jaramillo, J.; Gomperts, R.; Stratmann, R. E.; Yazyev, O.; Austin, A. J.; Cammi, R.; Pomelli, C.; Ochterski, J. W.; Ayala, P. Y.; Morokuma, K.; Voth, G. A.; Salvador, P.; Dannenberg, J. J.; Zakrzewski, V. G.; Dapprich, S.; Daniels, A. D.; Strain, M. C.; Farkas, O.; Malick, D. K.; Rabuck, A. D.; Raghavachari, K.; Foresman, J. B.; Ortiz, J. V.; Cui, Q.; Baboul, A. G.; Clifford, S.; Cioslowski, J.; Stefanov, B. B.; Liu, G.; Liashenko, A.; Piskorz, P.; Komaromi, I.; Martin, R. L.; Fox, D. J.; Keith, T.; Al-Laham, M. A.; Peng, C. Y.; Nanayakkara, A.; Challacombe, M.; Gill, P. M. W.; Johnson, B.; Chen, W.; Wong, M. W.; Gonzalez, C.; Pople, J. A. *GAUSSIAN 03*, revision C.02; Gaussian, Inc.; Wallingford, CT, 2004.

(20) (a) Landis, C. R.; Halpern, J. *J. Am. Chem. Soc.* **1987**, *109*, 1746. (b) Landis, C. R.; Feldgus, S. *Angew. Chem., Int. Ed.* **2000**, *39*, 2863.